Reaction Wheels Desaturation Using Magnetorquers and Static Input Allocation

Jean-François Trégouët, Denis Arzelier, Dimitri Peaucelle, Christelle Pittet, and Luca Zaccarian, *Senior Member, IEEE*

***Abstract*— Considering the most widely spread configuration of actuators for low orbit satellites, namely a set of reaction wheels and set of magnetorquers, we revisit the classical cross-product control law solution for achieving attitude stabilization and momentum dumping. We show how the classical solution has a quasi-cascade structure that, under a suitable input-to-state (ISS) assumption, can be stabilized by high gain, thereby making the actuators more inclined to saturate. Motivated by this, we propose a revisited version of this control law that transforms the quasi-cascade into a real cascade. Then, we show that both strategies are such that the attitude control is affected by the momentum dumping, and that they both require a suitable ISS property. To overcome these drawbacks, we propose a new allocation-based controller, which makes the attitude dynamics completely independent of the momentum dumping and induces global asymptotic stability without any ISS requirement. Several formal statements and simulation results support our discussions and highlight the pros and cons of the different control strategies.**

***Index Terms*— Aerospace control, attitude control, input allocation, Lyapunov methods, magnetorquers, reaction wheels desaturation.**

I. Introduction

THE attitude control problem has been a challenging issue for the scientific community for decades (see [1], [5], [23], [37], and references therein) and still constitutes an active area of research. Recently, the literature has been enriched by several remarkable solutions, which achieve asymptotic stability in a global way [25], [29]. If these results are an important step, they rely on an abstract context for which the availability of an external actuation torque is assumed. However, when it comes to physical realization of this control torque by means of real actuators, solutions mainly rely on engineering consideration and can be largely improved.

Most of three-axis stabilized spacecrafts are equipped with angular momentum storage devices, such as reaction wheels, when high pointing accuracy is required [7]. Despite their known advantages [38], these momentum exchange systems may suffer from saturation limitations as well as static friction when approaching zero angular velocity. Thus, reaction wheels need a secondary attitude control system for momentum unloading and desaturation of the reaction wheels system. For small satellites in low Earth orbits (LEO) magnetorquers provide a cheap, reliable, and effective external torque for momentum desaturation purposes [3], [4], [8], [26], [32]. Earth observation satellites such as Spot4, Jason1 and 2, Demeter, or as Corot for inertial pointing are thus equipped by magnetic and mechanical actuation systems [7], [27]. While reaction wheels are easily exploited because they can generate a torque in any desired direction at any time, magnetorquers rely on a more subtle principle: by generating a magnetic momentum that interacts with the geomagnetic field, a torque is created. However, as this field is not constant, due to the rotation of the satellite around the Earth, the synthesis models are naturally almost periodically time varying. In addition to that, at any given instant of time, the produced torque lies in the orthogonal plane to the instantaneous geomagnetic field leading to the noncontrollability of the direction parallel to the local geomagnetic field vector. For these reasons, the control problem associated with the magnetorquers is recognized as a challenging one [23], [26].

Despite these limitations, engineers frequently resort to this kind of actuators, for cost-effectiveness, efficiency, reliability, and weight reasons. Moreover, the combined action of the magnetorquers with the reaction wheels allows to regard the latter actuators as the main actuators for fine attitude control and the former ones as auxiliary actuators used for desaturation or momentum dumping. A classical engineering-based solution following this paradigm is the so-called cross-product control law mentioned in [3], [4], [8], and [32], where the problem is addressed within a linear approximation context.

In this paper, we address the problem of designing a suitable centralized law for the reaction wheels and magnetorquers on an inertially pointing satellite orbiting at low altitude. More precisely, given an attitude stabilizer that has been initially designed disregarding the momentum dumping problem, we propose a control scheme managing the two actuators in such a way that momentum dumping is performed continuously throughout the maneuver while remaining completely hidden

Manuscript received December 23, 2013; accepted April 13, 2014. Manuscript received in final form May 7, 2014. Recommended by Associate Editor A. Serrani.

J.-F. Trégouët is with the Laboratoire Ampère, Institut National des Sciences Appliquées de Lyon, Université de Lyon, Villeurbanne F-69621, France (e-mail: jeanfrancois.tregouet@insa-lyon.fr).

D. Arzelier and D. Peaucelle are with the Laboratoire d'analyse et d'architectures des Systèmescnrs, Centre National de la Recherche Scientifique, Toulouse F-31400, France, and also with the Laboratoire d'analyse et d'architectures des Systèmescnrs, Université de Toulouse, Toulouse F-31400, France (e-mail: arzelier@laas.fr; peaucelle@laas.fr).

C. Pittet is with the Centre National d'Etudes Spatiales, Toulouse F-31401, France (e-mail: christelle.pittet@cnes.fr).

L. Zaccarian is with the Laboratoire d'analyse et d'architectures des Systèmescnrs, Centre National de la Recherche Scientifique, Toulouse F-31400, France, Laboratoire d'analyse et d'architectures des Systèmescnrs, Université de Toulouse, Toulouse F-31400, France, and also with the Dipartimento di Ingegneria Industriale, University of Trento, Trento 38100, Italy (e-mail: lzaccarian@gmail.com).

Color versions of one or more of the figures in this paper are available online at http://ieeexplore.ieee.org.

Digital Object Identifier 10.1109/TCST.2014.2326037

for the attitude dynamics that exactly follows the response induced by the prescribed attitude stabilizer. This paper's contributions are summarized as follows.

First, our contribution is to provide a rigorous interpretation (inspired by the formalization of [23], where only magnetorquers are considered) of the architecture behind the cross-product control law. The treatment helps formalizing this approach by highlighting its hidden assumptions. Second, we propose a revisited version of the cross-product control law, which is shown to be valid in a wider range of practical situations. In particular, we show a peculiar feedback structure arising from this controller, which can be converted (using the proposed revisited law) into a more convenient cascaded form consisting of an upper subsystem whose state is the total angular momentum and a lower subsystem whose state is the satellite attitude (position and speed). We discuss and show by simulations that the above cascaded structure is not desirable due to the fact that the regulation of the angular momentum of the wheels perturbs the attitude control system. Third, our main contribution is then given and consists in a novel control scheme that is capable of reversing the cascaded scheme by way of static input allocation. Input allocation techniques address the problem of suitably assigning the low level actuators input, based on a higher level control effort requested by the control system [18]. Their use is especially suited in the presence of redundant plant inputs from the point of view of the main control task. Then, the allocation can be performed in such a way to optimize a cost function related to a lower priority secondary task (see [31] for an interesting collection of results in the aerospace, marine, and terrestrial vehicles). Within the attitude control setting described above, it appears natural to regard the primary goal as the attitude stabilization goal and the secondary goal as the reaction wheels desaturation goal. To this end, the employed allocation scheme may be selected as a static one (this is the structure of most of the existing techniques, well surveyed in [18]) or a dynamic one (following, e.g., the paradigm in [39] or the more recent developments in [11] and [30]). Note that the use of an allocation strategy for the engineering problem described here has been also proposed in [10]. However, the suggested distribution of the total control effort does not address the dynamics of the angular momentum of the wheels, which is instead the goal of the allocation scheme proposed in this paper.

In a nutshell, the allocation-based control scheme proposed here completely decouples the attitude stabilization task from the angular momentum of the wheels and is therefore capable of stabilizing the attitude dynamics following a prescribed law that can be designed disregarding the momentum dumping task. This goal is achieved by the cascaded structure of the new scheme where the upper subsystem, consisting in the (undisturbed) attitude stabilization loop, drives the lower subsystem, which performs the (lower priority) task of desaturating the reaction wheels. A preliminary version of this paper was presented in [35]. Here, as compared with [35], we treat a more general scenario with nonperiodic local geomagnetic fields, we provide several statements and proofs of the stability properties of the proposed schemes, and we provide revised and improved simulation tests based on realistic data from satellite missions.

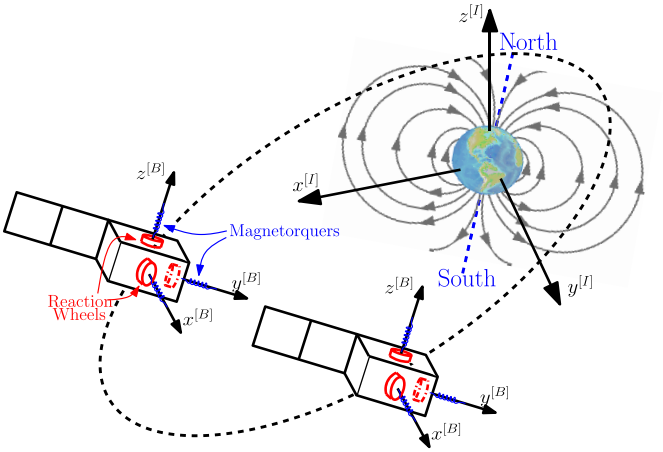

Fig. 1. Inertially pointing satellite orbiting around the Earth and equipped with reaction wheels and magnetorquers.

This paper is structured as follows. In Section II, we introduce the satellite model, some preliminary facts about global attitude stabilization, and formalize our problem statement. In Section III, we explain and interpret the cross-product control law, provide a revisited version of it, and establish its formal properties. In Section IV, we propose the new control strategy based on static allocation. In Section V, we provide comparative simulation results for the two controllers introduced in Sections III and IV. Finally, in Section VI, we give some concluding remarks.

Notation: Given any vectors $v, w \in \mathbb{R}^3$, the matrix $v^\times \in \mathbb{R}^{3\times 3}$ is a skew-symmetric matrix defined in such a way that the vector product between v and w satisfies $v \times w = v^\times w$

$$v^\times = \begin{bmatrix} 0 & -v_z & v_y \\ v_z & 0 & -v_x \\ -v_y & v_x & 0 \end{bmatrix} \text{ for } v = \begin{bmatrix} v_x & v_y & v_z \end{bmatrix}^T.$$

The identity quaternion is denoted by $q_\circ = [0 \;\; 0 \;\; 0 \;\; 1]^T$. The set $\mathbb{R}_{\geq 0}$ denotes the non-negative reals while $\mathbb{Z}_{\geq 0}$ denotes the non-negative integers. The identity matrix of size $n \times n$ is written $\mathbf{1}_n$. Depending on its argument, the bars $|\cdot|$ refer to the absolute value of a scalar, the Euclidean norm of a vector, or the induced l_2/spectral-norm of a matrix. The superscript $^{[I]}$ indicates that the related vector is expressed in the inertial frame. Otherwise, the body-fixed frame is considered.

II. Preliminaries and Problem Statement

Fig. 1 represents the scenario addressed in this paper, namely an inertially pointing satellite equipped with two actuator sets:

1) the reaction wheels that are capable of exerting a triple of torques spanning all the degrees of freedom of the attitude dynamics but suffer from the drawback of possibly experiencing a gradual increase of their spinning speed, due to their inability to alter the total momentum of the satellite affected by external disturbances;
2) the magnetorquers that are capable of exerting a rank deficient torque on two out of the three degrees of freedom of the attitude dynamics due to the fact that they

interact with the geomagnetic field; this second actuator may affect the total momentum of the satellite and therefore can be used to suitably stabilize the rotational speed of the wheels, even though the rank deficient nature of the generated torque is a challenge to be addressed.

Within the above context, we address in this paper the goal of suitably using the redundancy available in the two sets of actuators to stabilize the attitude of the satellite while simultaneously regulating the rotational speed of the wheels (momentum dumping). Note that attitude stabilization and momentum dumping are potentially conflicting goals because attitude control requires to speed up (or decelerate) the wheels, which may badly interact with the momentum dumping performed by the magnetorquers. From an engineering standpoint, the problem addressed and solved in this paper can be formulated as follows.

Problem 1: Given a spacecraft equipped with reaction wheels and magnetorquers actuators, as represented in Fig. 1, design a control strategy for driving the two sets of actuators to ensure simultaneously that the body frame is aligned with the inertial frame (attitude stabilization) and that the angular momenta of the reaction wheels are stabilized at a given reference value.

As customary in the case of redundancy of actuators, the engineering problem described in Problem 1 is usually addressed in two steps. First, a suitable attitude stabilizer with respect to given attitude specifications is obtained. It is based on an abstract model that does not take the reaction wheels saturation issue into account. Then, an additional control layer, implementing this control law for the retained actuation equipment, is designed. We stress that this paper is mainly concerned with the second step. Thus, all our derivations are valid for any stabilizer as long as it satisfies some mild regularity properties. Nevertheless, for illustration purposes, and to show the potential of our scheme to provide global results on nonlinear models, we use the attitude controller proposed in [25].

To suitably address and solve Problem 1, we give in this section the essential material to formulate it in mathematical terms. First, the dynamics of the satellite model are described in Section II-A. Then, in Section II-B, we recall the global attitude stabilizer proposed in [25] and prove some additional properties that were not given in [25]. Then, in Section II-C, we introduce some assumptions on the satellite orbit that enable us, together with the other derivations of the section, to mathematically formalize the engineering Problem 1.

A. Attitude Equations for an Inertially Pointing Satellite With Reaction Wheels and Magnetorquers

The total angular momentum of the satellite in the body-fixed frame comprises the angular momentum $J\omega$ of the central body and the angular momentum h_w of the reaction wheels

$$h_T = J\omega + h_w \tag{1}$$

where $\omega \in \mathbb{R}^3$ and $J \in \mathbb{R}^{3\times 3}$ are the rotational speed of the satellite body-fixed frame with respect to the inertial frame and the symmetric matrix corresponding to its moment of inertia, respectively. Applying Newton's theorem in the inertial frame, we get

$$\dot{h}_T^{[I]} = T_m^{[I]} \tag{2}$$

where $T_m^{[I]}$ is the torque generated by the magnetorquers and acting as an external torque on the spacecraft. When expressed in the body-fixed frame, (2) becomes

$$\dot{h}_T + \omega^\times h_T = T_m \tag{3}$$

where the gyroscopic term $\omega^\times h_T$ appears due the rotation of the body-fixed frame with respect to the inertial frame. Replacing h_T in (3) by its expression given in (1) and recognizing that the variation of h_w corresponds to the torque τ_w applied by the reaction wheels, with straightforward manipulations, we get the dynamic equations in the body-fixed frame

$$\begin{cases} J\dot{\omega} + \omega^\times(J\omega + h_w) = -\tau_w + T_m \\ \dot{h}_w = \tau_w. \end{cases} \tag{4a}$$

The attitude of the spacecraft is conveniently described using quaternion coordinates

$$q = \begin{bmatrix} \varepsilon \\ \eta \end{bmatrix} \in \mathbb{S}^3$$

where $\varepsilon \in \mathbb{R}^3$ and $\eta \in \mathbb{R}$. By definition, the three-sphere $\mathbb{S}^3$ refers to the set of every element $q \in \mathbb{R}^4$ satisfying the constraint $|q| = 1$. For an inertially pointing satellite, the quaternion q characterizes the instantaneous rotation of the body-fixed frame with respect to the inertial frame. The angular position dynamics is then described by the following well-known kinematic differential equation [19]:

$$\dot{q} = F(\omega)q = \frac{1}{2}\begin{bmatrix} -\omega^\times & \omega \\ -\omega^T & 0 \end{bmatrix}, \quad q = \frac{1}{2}\begin{bmatrix} -\omega^\times\varepsilon + \eta\omega \\ -\omega^T\varepsilon \end{bmatrix} \tag{4b}$$

where $F(\omega)$ is clearly a skew-symmetric matrix.

The magnetic torque T_m produced by the magnetorquers originates from the interaction between the local geomagnetic field $\tilde{b}$ and magnetic momentum.[1] τ_m according to the following relationship $T_m = -\tilde{b}^\times\tau_m$. Then, the magnetic field $\tilde{b}$ is a function of both the location of the spacecraft along its orbit and its attitude. These two dependences can be separated out writing $\tilde{b}$ as $R(q)\tilde{b}_\circ$, where $R(q)$ is the rotation matrix expressing the body-fixed frame with respect to the inertial frame, whose expression clearly depends on the quaternion q, and $\tilde{b}_\circ$ is the geomagnetic field expressed in the inertial frame

$$T_m = -(R(q)\tilde{b}_\circ(t))^\times\tau_m. \tag{4c}$$

An explicit expression of $R(q)$ can be written as follows [16]:

$$R(q) = (\eta^2 - \varepsilon^T\varepsilon)I_3 + 2\varepsilon\varepsilon^T - 2\eta\varepsilon^\times. \tag{4d}$$

Under the assumption that the orbital trajectory is perfectly known, the time evolution of $\tilde{b}_\circ(t)$ can be predicted using a model of the geomagnetic field, such as the International Geomagnetic Reference Field (IGRF), which gives access to the local magnetic field at any point in space [38].

[1]The dynamics of magnetic coils can be neglected as it reduces to a very fast electrical transient [22].

B. Global Asymptotic Stabilization of the Attitude Dynamics

In this paper, we will address control design problems for model (4) derived in Section II-A aiming at global asymptotic stabilization of the attitude dynamics. This problem can be understood as the problem of designing a feedback controller from (ω, q) capable of globally[2] asymptotically stabilizing a suitable equilibrium for the simpler model given by (4b) and

$$J\dot{\omega} + \omega^{\times} J\omega = u + d \tag{5}$$

from the control input u. The disturbance input d will be useful later and should be considered as zero for stability purposes.

Despite its apparent simplicity, this problem involves tricky aspects that have been highlighted in [1]. The main conclusion is that there exists no continuous time-invariant (static or dynamic) controller that globally asymptotically stabilizes a desired equilibrium attitude. This property is related to the fact that every continuous time-invariant closed-loop vector field on SO(3), the set of attitudes of a rigid body, has more than one closed-loop equilibrium, and hence, the desired equilibrium cannot be globally attractive [1].

However, as soon as the control law is not continuous or time-invariant, this obstruction does not hold anymore and many remarkable solutions to the global attitude stabilization problems have been given in [29] and references therein. In this paper, we will use a dynamic (discontinuous) hybrid controller that was recently proposed in [25], whose dynamical equation can be written as follows using the notation in [13], [14]:

$$\begin{aligned} \dot{x}_c &= 0, \quad (q, \omega, x_c) \in C \\ x_c^+ &= -x_c, \quad (q, \omega, x_c) \in D \\ u &= -c x_c \varepsilon - K_\omega \omega \end{aligned} \tag{6a}$$

where the flow set C and the jump set D are defined as

$$\begin{aligned} C &:= \{(q, \omega, x_c) \in \mathbb{S}^3 \times \mathbb{R}^3 \times \{-1, 1\} : x_c \eta \geq -\delta\} \\ D &:= \{(q, \omega, x_c) \in \mathbb{S}^3 \times \mathbb{R}^3 \times \{-1, 1\} : x_c \eta \leq -\delta\}. \end{aligned} \tag{6b}$$

Note that the scalar controller state x_c is constrained to belong to the set $\{-1, 1\}$ by the hybrid dynamics. Moreover, the control input u corresponds to a state feedback from (ω, ε), where the sign of the ε gain is toggled by x_c. The suggestive result of [25] is that the hybrid controller (6) is able to asymptotically stabilize the set (attractor) $\mathcal{A} \subset \mathbb{S}^3 \times \mathbb{R}^3 \times \{-1, 1\}$ defined as

$$\mathcal{A} = \{q_\circ\} \times \left\{ \begin{bmatrix} 0 \\ 0 \\ 0 \end{bmatrix} \right\} \times \{1\} \bigcup \{-q_\circ\} \times \left\{ \begin{bmatrix} 0 \\ 0 \\ 0 \end{bmatrix} \right\} \times \{-1\} \tag{7}$$

which is the union of two points, corresponding to $q = q_\circ$ and $q = -q_\circ$, respectively. Remarkably, due to the well-known double coverage nature of quaternion coordinates (see [5]), these two points correspond to the same element of SO(3), i.e., the same attitude of the satellite. The following lemma states the global asymptotic stability result of [25] with an additional local exponential stability property, which will be useful later in this paper.

Lemma 1: For any positive definite matrix $K_\omega = K_\omega^T \succ 0$ and scalars $c > 0$, $\delta \in (0, 1)$, the closed-loop given by (4b) and (5) with $d = 0$ and (6) is such that the set $\mathcal{A}$ in (7) is globally asymptotically stable (GAS) and locally exponentially stable (LES).

Proof: The proof of GAS is established in [25, Th. 4.2]. To show LES, first recall from [25] that all solutions to (4b), (5), and (6) (with $d = 0$) are eventually continuous, indeed as noted in [25, top of page 2525], for a suitable Lyapunov function V, one has $V^+ - V = -4\delta$ and since V is non-negative, there cannot be any jump in the neighborhood of $\mathcal{A}$ where $V < 4\delta$. Therefore, we study LES by only focusing on the flow dynamics and continuous-time LES bounds. Moreover, since the two points in $\mathcal{A}$ are disjoint, then local analysis amounts to analyzing separately the two points (note that since no jumps occur locally, then x_c remains constant along local solutions). We carry out the analysis looking at the left one in (7), namely $x_\circ = (q_\circ, 0, 1)$. The other one follows the same steps and is omitted.

Consider now that the motion in $\mathbb{S}^3$ can be studied in the variables ε, ω replacing η by its constrained value $\eta = (1 - \varepsilon^T \varepsilon)^{1/2}$ (note also that η is positive around the equilibrium $x_\circ$). Then, we can replace (4b) by

$$\dot{q} = \frac{1}{2} \begin{bmatrix} -\omega^{\times} \varepsilon + \sqrt{1 - \varepsilon^T \varepsilon}\, \omega \\ -\omega^T \varepsilon \end{bmatrix}$$

and the linearized dynamics around the equilibrium $x_\circ$ corresponds to

$$\begin{bmatrix} \dot{\varepsilon} \\ \dot{\omega} \end{bmatrix} = \begin{bmatrix} 0 & 1/2 \cdot \mathbf{1}_3 \\ -cJ^{-1} & -J^{-1} K_\omega \end{bmatrix} \begin{bmatrix} \varepsilon \\ \omega \end{bmatrix}$$

which is exponentially stable[3] for any positive c and positive definite K_ω. As a consequence, from the linear approximation theorem (see [20, Th. 4.7]), the equilibrium is LES, namely there exist positive scalars Υ, λ such that for small enough initial conditions, $|(\varepsilon(t), \omega(t))| \leq \Upsilon \exp(-\lambda t) |(\varepsilon(0), \omega(0))|$ for all $t \geq 0$. Assume now that $\varepsilon(0)$ is small enough so that $\eta(t) = (1 - \varepsilon(t)^T \varepsilon(t))^{1/2} > 0$ for all $t \geq 0$. Then, one can write

$$\begin{aligned} |1 - \eta| &= (1 - \eta) \leq (1 + \eta)(1 - \eta) = 1 - \eta(t)^2 \\ &= \varepsilon(t)^T \varepsilon(t) \leq \Upsilon^2 \exp(-2\lambda t) |(\varepsilon(0), \omega(0))|^2 \end{aligned}$$

which gives the local exponential bound also for the variable η and completes the proof of LES. ■

Remark 1: One of the reasons why we adopt the hybrid stabilizer of [25] is that the lack of robustness of a nonhybrid stabilizer, together with the so-called unwinding effect (see [25, §2] for details) is successfully overcome by the hybrid scheme, in light of the results of [14, Ch. 7]. In particular, since all the data of the hybrid solutions proposed here satisfy the basic assumptions of [14] and the attractor (7) is

[2]Note that we actually consider a strict subset of $\mathbb{R}^7$, since $q^T q = 1$ holds for all times, and thus we shall call this property asymptotic stability in the large rather than global asymptotic stability [21], however, for consistency with existing results, such as [1] and [25], we use global asymptotic stability throughout this paper.

[3]This fact is easily proven using the Lyapunov function $V = 2c\varepsilon^T \varepsilon + \omega^T J \omega$, which satisfies $\dot{V} = -2\omega^T K_\omega \omega$, and applying La Salle's invariance principle.

compact, then by applying [14, Lemma 7.20 and Th. 7.21], asymptotic stability is robust to small disturbances and semiglobally practically robust to large ones. In particular, according to the definition in [14, Definition 7.18], all solutions to the dynamical system generated by perturbing the right-hand side of the differential equation remain arbitrarily δ-close to the attractor (7) as long as they start in a Δ-ball around it, where as the size of the disturbance shrinks, one can show that δ becomes arbitrarily small (practical) and Δ becomes arbitrarily large (semiglobal). For more details, the reader is referred to [14]. ∘

Throughout this paper, we will consider the attitude stabilizer (6) for the spacecraft dynamics. However, we stress that the results presented here are valid for any static or dynamic stabilizer inducing GAS and LES of the attractor $\mathcal{A}$ in (7).

C. Mathematical Formalization of the Design Goal

While the stabilization result in Lemma 1 should be regarded as an important step toward the stabilization of dynamics (4), it is still not implementable for that dynamics as the availability of u is an abstraction. Indeed, global asymptotic stabilization of a suitable attractor for (7) requires to reach the attitude equilibrium and to dump the momentum h_w of the reaction wheels. If using the magnetorquers for this secondary task, complication arises from the fact that magnetorquers are associated with tricky time-varying controllability problems. Indeed, at any given instant time, the achievable torque T_m is constrained to a plane because the vector T_m arises from the cross product between τ_m and $\tilde{b}$ and therefore is always orthogonal to $\tilde{b}$. The fact that the 3×3 matrix $\tilde{b}^\times$ is structurally singular originates from this remark. For this reason, the preliminary feedback

$$\tau_m = \frac{\tilde{b}^\times}{|\tilde{b}|^2} u_m \tag{8}$$

is often used and introduces the new control vector $u_m \in \mathbb{R}^3$ (see [23] and references therein) so that the resulting torque T_m is equal to $-\tilde{b}^\times \tilde{b}^\times / |\tilde{b}|^2 u_m$. In such a case, the identity $-\tilde{b}^\times \tilde{b}^\times / |\tilde{b}|^2 = \mathbf{1}_3 - \tilde{b}\tilde{b}^T / |\tilde{b}|^2$ allows to interpret T_m as the projection of u_m on the orthogonal plane to $\tilde{b}$. Thus, the control action (8) normalizes the magnetic field $\tilde{b}$ and reduces the control effort by canceling out the useless part of u_m, which is in the direction of $\tilde{b}$.

Despite these limitations, strong controllability properties still exist whenever $\tilde{b}(t)$ is time varying[4] and exhibits a sufficiently rich behavior in such a way to being capable of persistently spanning all of the 3-D space. Sufficient properties for the time-varying function $t \mapsto \tilde{b}(t)$ to be able to preserve this controllability can be expressed in terms of the following matrix:

$$\Pi(t) = \frac{1}{t} \int_0^t b_\circ(\tau) b_\circ^T(\tau) d\tau \tag{9}$$

where $b_\circ(t) = \tilde{b}_\circ(t) / |\tilde{b}_\circ(t)|$ is the normalized expression of the geomagnetic field in the inertial frame. These properties are formalized in the next assumption and suitably commented next.

Assumption 1: Given the matrix function $t \mapsto \Pi(t)$ in (9), the following limit exists, is finite and satisfies:

$$\Pi_\infty = \lim_{t \to +\infty} \Pi(t), \quad \Pi_\infty \prec \mathbf{1}_3. \tag{10}$$

Moreover, there exists a scalar $\sigma > 0$ such that

$$|M(t)| = |t(\Pi(t) - \Pi_\infty)| \leq \sigma \quad \forall t \geq 0. \tag{11}$$

It is interesting to remark that if $b_\circ(\tau)$ is a signal having finite power then Assumption 1 is verified [40, Ch. 4].

Remark 2: In [35], we imposed a stronger assumption on the magnetic field $b_\circ$ because we required it to be periodic with half of the period T_0 of the orbital motion of the spacecraft. In that specific case, the limit in (10) exists and corresponds to $\Pi_\infty = \int_0^{T_0/2} b_\circ(\tau) b_\circ^T(\tau) d\tau$ and then boundedness of $M(t)$ can be established by noticing that $\Pi(kT_0/2) = \Pi_\infty$ for each $k \in \mathbb{Z}$ and using boundedness of $b_\circ$. Here, we impose milder assumptions on $b_\circ$ also in light of the data reported later in Fig. 5, where the actual evolution of $b_\circ$ along several orbits is compared to its periodic approximation.

It is also worthwhile to mention that our Lyapunov construction is inspired by [23], where only the following assumption is made on the geomagnetic field $b_\circ$ (see the first displayed equation in [23, Lemma 1]):

$$\bar{\Gamma}_0 = \lim_{T \to +\infty} -\frac{1}{T} \int_0^T b_\circ^\times(\tau) b_\circ^\times(\tau) d\tau, \quad 0 < \bar{\Gamma}_0 < \mathbf{1}_3. \tag{12}$$

Property (12) is weaker than Assumption 1 and corresponds to only enforcing relation (10), as one can easily check by selecting $\bar{\Gamma}_0 = \mathbf{1}_3 - \Pi_\infty$. In [23, Proof of Proposition 1], it is claimed that under the assumption that $|b_\circ(t)| = 1$ for all $t \geq 0$, (12) is sufficient for the existence of $\sigma > 0$ satisfying (11). Nevertheless, selecting

$$b_\circ(t) = \frac{1}{2(t+1)} \begin{bmatrix} t+2 \\ \sqrt{3t^2+4t} \sin(t) \\ \sqrt{3t^2+4t} \cos(t) \end{bmatrix}$$

it is possible to prove that (12) [equivalently, (10)] holds while there exists no $\sigma > 0$ satisfying (11). The proof of this fact is given in the appendix of [36]. Since we follow the construction of [23, Proposition 1] in our Lyapunov derivations, in light of this example, we explicitly enforce (11) in our Assumption 1. Note that the example above does not clearly correspond to a plausible physical scenario and arises from a purely mathematical observation. Finally, we should emphasize that the result in [23, Proposition 1] has been proven later in [24] under milder assumptions and with a different proof technique. Here, we use the Lyapunov-based proof technique of [23] that can be effectively employed in our context. ∘

Based on Assumption 1, we can now mathematically formalize the engineering problem stated in Problem 1 dealing with the implementation of the attitude controller presented in Section II-B to suitably stabilize the spacecraft dynamics presented in Section II.

Problem 2: Consider the spacecraft described by (4) and satisfying Assumption 1. Design a state-feedback controller acting on the input (τ_w, τ_m), which ensures global asymptotic

[4]Note that it is also possible to achieve three-axis stabilization using only magnetorquers, as demonstrated in [23]. However, only poor attitude control performance can be expected when using this type of solution because of the very nature of these singular actuators.

stability of the set $\mathcal{A} \times \{h_w \in \mathbb{R}^3 : \ h_w = h_{\text{ref}}\}$, where $\mathcal{A}$ is defined in (7) and $h_{\text{ref}} \in \mathbb{R}^3$ is any constant setpoint reference for the angular momentum h_w of the reaction wheels.

III. Classical Approach Revisited

As a first contribution of this paper, a rigorous mathematical treatment of the so-called cross-product control law is proposed in Sections III-A and III-B before introducing a revisited version of this control law in Section III-C.

A. Classical Cross-Product Control Law

A classical approach to the solution to Problem 2 is the so-called cross-product control law well surveyed in [3], [4], [8], and [32]. This control law has been used, e.g., in the spacecraft Demeter [27], as described in [28]. The underlying philosophy of this approach is to use the reaction wheels actuator for the attitude stabilization loop, whereas the momentum of the wheels is simultaneously regulated by a second control loop acting on the magnetorquers. This leads to two control loops designed independently, as illustrated next.

1) Attitude Stabilization Loop: For attitude stabilization, one can rewrite the first relationship in (4a) as

$$J\dot{\omega} + \omega^\times J\omega = \underbrace{-\tau_w - \omega^\times h_w}_{u} + \underbrace{T_m}_{d}. \tag{13}$$

Note that (13) corresponds to (5) with $u = -\tau_w - \omega^\times h_w$ and $d = T_m$. Then, forgetting for a moment, the presence of the disturbance d (which should however, be taken into account at a later stage for stability analysis), the reaction wheels input τ_w can be selected by only focusing on the attitude control goal using some global asymptotic stabilizer, such as the one discussed in Section II-B. In particular, with that construction one can use (6) for u and

$$\tau_w = -\omega^\times h_w - u. \tag{14}$$

Then, Lemma 1 implies that attitude stabilization is achieved globally, with $d = 0$.

2) Momentum Dumping Loop: For the task of controlling h_w, assume that the attitude controller is capable of converging to (a small enough neighborhood of) the desired equilibrium attitude $(q, \omega) \in \mathcal{A}$ given in (7). The equilibrium, $u + T_m = 0$ gives $\tau_w = T_m$, for $(q, \omega) \in \mathcal{A}$. Then, remembering that h_{ref} is constant, from the second equation in (4a) and from (4c), we get for $(q, \omega) \in \mathcal{A}$

$$\dot{h_w - h_{\text{ref}}} = -\tilde{b}^\times(t)\tau_m. \tag{15}$$

One can then select the magnetorquers input τ_m in such a way to stabilize the origin of (15) following, for example, the so-called cross-product control law of [3], [4], [8], and [32], corresponding to

$$\tau_m = -\frac{\tilde{b}^\times(t)}{|\tilde{b}(t)|^2} k_p (h_w - h_{\text{ref}}) \tag{16}$$

which can be interpreted as the combination of the preliminary feedback (8) with a proportional action $k_p(h_w - h_{\text{ref}})$. It can be shown that this control law globally exponentially stabilizes the attractor

$$\mathcal{A}_h = \{h_w \in \mathbb{R}^3 : \ h_w = h_{\text{ref}}\} \tag{17}$$

as stated in the following lemma whose proof, given in the Appendix, follows the same steps as in [23, Proposition 1].

Lemma 2: If Assumption 1 holds, then for any scalar $k_p > 0$, the set $\mathcal{A}_h$ in (17) is globally exponentially stable for the closed-loop system (15), (16) with $\tilde{b}$ replaced by $\tilde{b}_\circ$.

Remark 3: Following the same philosophy, other control laws have been proposed in the literature to achieve momentum dumping by focusing on (15). For example, in [22], a periodic linear quadratic controller has been designed relying on numerical methods to solve the periodic Riccati equation. Moreover, a semianalytical optimal open-loop solution for only one axis was proposed in [12]. ∘

B. Quasi-Cascade Structure of the Classical Approach

A closer look at the cross-product control law strategy reveals that the attitude stabilization loop (14) is designed assuming that the second loop is at the equilibrium [namely $h_w = h_{\text{ref}}$, which induces $d = T_m = 0$ according to (16) and to (4c)]. Conversely, the momentum dumping action (16) is designed assuming that the first loop is at the equilibrium [$q = q_\circ$ so that $\tilde{b} = R(q)\tilde{b}_\circ$ is replaced by $\tilde{b}_\circ$ in (15) and (16)]. Despite its intuitive interpretation, it seems that formally showing desirable stabilization properties of the overall controller (6), (14), (16) is not so straightforward. Some directions are given with respect to this in [3], [4], [6], [9], [15], and [22], where a frequency separation argument is required between the two loops cited above, which corresponds to selecting a very aggressive action of the attitude stabilizer (14). This can be performed, for example, by selecting sufficiently large gains c and K_ω in (6).

One way to tackle the asymptotic stability properties of the equilibrium set $\mathcal{A} \times \mathcal{A}_h$ [see (7) and (17)] for the overall dynamics (4), (6), (14), (16) is to recognize that the input τ_w to the reaction wheels does not change the total angular momentum $h_T^{[I]} = R^T(q)(J\omega + h_w)$ [this follows easily from (1) and (2) and is obvious from the fundamental mechanics viewpoint]. Thus, in order to help separating the influence of each actuator, it makes sense to use $h_T^{[I]}$, rather than h_w to represent the momenta of the reaction wheels in the first loop. Indeed, in the set $\mathcal{A} \times \mathcal{A}_h$, one has $h_T^{[I]} = R^T(\pm q_\circ)h_w = h_w$. However, when substituting h_w by $R(q)h_T^{[I]} - J\omega$ in the cross-product control law (16), bearing in mind that k_p is a scalar, $(Rv)^\times = Rv^\times R^T$ for all $v \in \mathbb{R}^3$ and $|\tilde{b}| = |\tilde{b}_\circ|$, one gets

$$\begin{aligned}
\tau_m &= -\frac{(R(q)\tilde{b}_\circ(t))^\times}{|\tilde{b}(t)|^2} k_p \big(R(q)h_T^{[I]} - J\omega - h_{\text{ref}}\big) \\
&= -R(q)\frac{\tilde{b}_\circ^\times(t)}{|\tilde{b}_\circ(t)|^2} R^T(q) k_p R(q)\big(h_T^{[I]} \\
&\quad - R^T(q)\,(J\omega + h_{\text{ref}})\big) \\
&= -R(q)\frac{\tilde{b}_\circ^\times(t)}{|\tilde{b}_\circ(t)|^2} k_p \Big(h_T^{[I]} - h_{\text{ref}} \\
&\quad + R^T(q)\Big(\underbrace{(R(q) - \mathbf{1}_3)h_{\text{ref}} - J\omega}_{\zeta(q,\omega)}\Big)\Big).
\end{aligned} \tag{18}$$

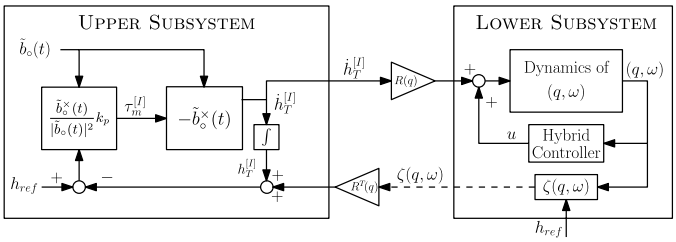

Fig. 2. Quasi-cascaded structure of the cross-product control law and the role of the signal $\zeta(q,\omega)$.

Equation (18) provides insightful understanding about the quasi-cascaded, or feedback structure of the cross-product control law, which, based on (18), can be remapped in the inertial coordinate frame to get

$$\tau_m^{[I]} = -\frac{\tilde{b}_\circ^\times(t)}{|\tilde{b}_\circ(t)|^2} k_p \big(h_T^{[I]} - h_{\text{ref}} + R^T(q)\zeta(q,\omega)\big). \quad (19)$$

This is clarified in the block diagram of Fig. 2, where the presence of the signal $\zeta(q,\omega)$ creates an undesirable dependence of $\dot{h}_T^{[I]}$ on the attitude parameters (q,ω). Even though the literature contains reference to frequency separation (or two time scale results when speaking in nonlinear terms), it is unclear how to apply those results to the scheme of Fig. 2, where the time-varying input $\tilde{b}_\circ(t)$ makes it hard to say that the upper subsystem is slower than the lower one. Conversely, a possible way to establish asymptotic stability of the attractor is via the input-to-state (ISS) small gain approach [17], where one could claim that increasing the gain of the attitude stabilizer in the lower subsystem allows to reduce enough the ISS gain from $h_T^{[I]}$ to $R^T(q)\zeta$ in the block diagram. Then, one could characterize the cross-product control law solution as some sort of high-gain feedback solution leading to global asymptotic stabilization of the set $\mathcal{A}\times\mathcal{A}_h$ defined in (7) and (17) via small gain results.

C. Revisited Cross-Product Control Law

While the cross-product control law approach of the previous section has been long used in experimentation and performs desirably when a high-gain attitude stabilization is adopted, the natural question that arises in light of (18) is whether the signal $\zeta(q,\omega)$ is really necessary. The answer is no, if one recalls that the stabilizer (16) was designed by focusing on the case $(q,\omega)\in\mathcal{A}$ and that in this set one has $\zeta(q,\omega)=0$. Consequently, this signal ζ can be freely inserted into (16) to obtain the revisited cross-product control law

$$\tau_m = -\frac{\tilde{b}^\times(t)}{|\tilde{b}(t)|^2} k_p (h_w - h_{\text{ref}} - \zeta(q,\omega)) \quad (20a)$$

which can be used as an alternative to stabilizer (16). The advantage of using the revisited law (20a) in place of the classical one (16) is best appreciated by rewriting (20a) as follows, by using the identities in (18):

$$\tau_m^{[I]} = -\frac{\tilde{b}_\circ^\times(t)}{|\tilde{b}_\circ(t)|^2} k_p \big(h_T^{[I]} - h_{\text{ref}}\big). \quad (20b)$$

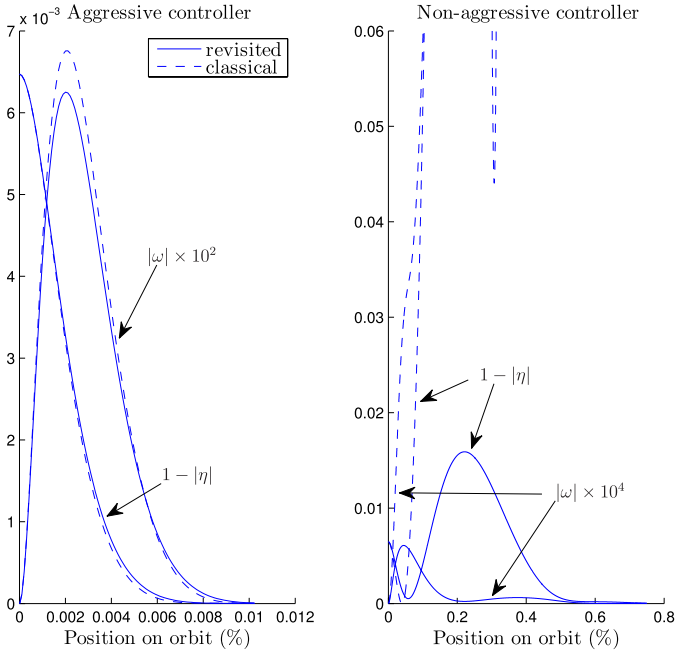

Fig. 3. Comparison in Remark 4 between the classical (dashed) and revisited (solid) cross-product control laws when using an aggressive attitude controllers (left-hand side plot) and a nonaggressive one (right-hand side plot).

Remark 4: From an engineering viewpoint, the revisited control strategy given by (6), (14), and (20) is not much different from the classical cross-product control law (6), (14), (16) whenever the attitude stabilizer is aggressive enough so that the standing assumptions behind this historical approach are respected. However, significant differences are witnessed when using nonaggressive actions in the attitude controller and this mainly because while the revisited solution keeps performing desirably, the classical solution exhibits very large overshoots and even diverging responses. This can be motivated by the fact that the interaction between the momentum dumper (upper subsystem) and the attitude stabilizer (lower subsystem) in Fig. 2 does not anymore satisfy a small gain condition and asymptotic stability is lost.

Fig. 3 illustrates this fact by comparatively showing the responses of the two closed-loops starting from the initial conditions $w_0=\mathbf{0}$, $q_0=[0.10,0.05,0.02,0.99]^T$, $h_{w0}=[0.09,0.072,0.078]^T$, and $x_{c_0}=1$. For illustration purposes, the simulations of Fig. 3 have been carried out without imposing any saturation limits on τ_w and τ_m, so that the difference among the two dynamic solutions can be best appreciated. Simulations incorporating these saturations are carried out in Section V. In the figure, the dashed lines correspond to the response obtained from the classical solution (6), (14), (16) and the solid lines correspond to the revisited law (6), (14), and (20). With these two controllers, two cases are analyzed: the left-hand side plot shows the responses obtained when using an aggressive attitude controller, corresponding to $K_w=5\cdot\mathbf{1}_3$ and $c=0.5$ while the right plot corresponds to the less aggressive gains $K_w=0.07\cdot\mathbf{1}_3$ and $c=10^{-4}$. In both cases, we consider $\delta=0.5$ and $k_p=0.01$. We illustrate the closed-loop responses by showing

the (rescaled) norm of the angular speed and the scalar value $1 - |\eta|$, which is zero in the attractor. Similar comparison results are experienced when looking at all the components of the state (q, ω, x_c, h_w). Note that the responses of the two closed loops are essentially the same in the case when the classical solution performs desirably, but the revisited solution preserves asymptotic convergence to the attractor, with the less aggressive attitude stabilizer. ∘

One advantage arising from replacing (16) by (20) is that the feedback interconnection of Fig. 2 becomes a cascaded interconnection (the dashed arrow disappears) and one can then use results on stability of cascaded nonlinear systems to establish global asymptotic stability of the set $\mathcal{A} \times \mathcal{A}_h$ defined in (7) and (17). In particular, for the cascaded system of Fig. 2, the upper subsystem regulates the total angular momentum using the magnetorquers and is completely independent from the satellite attitude and lower subsystem regulates the attitude dynamics using the reaction wheels and is disturbed by the upper subsystem through the action of $d = T_m = -R(q)\tilde{b}_\circ(t)^\times \tau_m^{[I]}$. More specifically, the overall closed loop corresponds to the revisited cross-product control law (6), (20) together with

$$\dot{h}_T^{[I]} = -\tilde{b}_\circ(t)^\times \tau_m^{[I]} \tag{21a}$$

$$\begin{cases} \text{(4b)} \\ J\dot{\omega} + \omega^\times J\omega = u + R(q)\dot{h}_T^{[I]}. \end{cases} \tag{21b}$$

Using the result established by Lemma 2, which can be rewritten in the same form when looking at the feedback (21a) and (20b), one gets global exponential stability of the upper subsystem. Then, global asymptotic stability can be derived from properties of cascaded interconnections of hybrid systems (recall that the attitude controller is hybrid). The result is formalized in the following theorem.

Theorem 1: Under Assumption 1, given any set of gains $k_p > 0$, $K_\omega = K_\omega^T \succ 0$, $c > 0$, and $\delta \in (0, 1)$, consider the closed-loop system between plant (4) and controller (6), (14), (20a) with state space variables $x = (q, \omega, x_c, h_w)$. Then, the set $\mathcal{A}_e = \mathcal{A} \times \mathcal{A}_h$ as defined in (7) and (17) is locally asymptotically stable.

Moreover, if the hybrid closed-loop system (4b), (5), (6) is ISS from the input d (in the sense of [2]), then the set $\mathcal{A}_e$ is GAS, namely the control scheme solved the formalization in Problem 2 of the engineering Problem 1.

Proof: First, let us represent the closed-loop with the coordinates $\bar{x} = (q, \omega, x_c, h_T^{[I]})$ and note that, from (1) and $h_T^{[I]} = R^T(q)h_T$, we have $x \in \mathcal{A}_e$ if and only if $\bar{x} \in \mathcal{A}_e$. Then, we can prove the theorem by studying asymptotic stability of $\mathcal{A}_e$ for the transformed dynamics (6), (20b) (21), which is in cascaded form.

For this cascade, using Lemma 2 rewritten by replacing h_w by $h_T^{[I]}$, the set $\mathcal{A}_h$ is globally exponentially stable for the upper subsystem, corresponding to (21a) and (20b). Moreover, the lower subsystem with zero input, corresponding to (6), (21b) with $\dot{h}_T^{[I]} = 0$, coincides with (4b), (5), and (6) with $d = \mathbf{0}$ and therefore guarantees global asymptotic stability (and local exponential stability) of the set $\mathcal{A}$ from Lemma 1. Then, we can apply [13, Corollary 19] and the follow-up results about the cascades [13, (23)] to prove local asymptotic stability of the cascade.[5] Moreover, if the lower subsystem is ISS stable with respect to d in the sense of [2], then all solutions are bounded for any initial condition. Then, the result follows once again from the results on cascaded system stated for [13, (23)]. ■

IV. Using Static Allocation to Invert the Cascade

The solution to Problem 2 presented in the Section III can lead to satisfactory closed-loop responses, however, it suffers from three main drawbacks.

1) Due to the cascaded structure of Fig. 2, the attitude control loop is undesirably disturbed by the momentum dumping system. Since attitude control is more important than momentum dumping, it would be more desirable if the converse relation was in place.
2) Global asymptotic stability is only established by Theorem 1 under an ISS assumption on the attitude control system, which is not easy to guarantee in general. It would be more desirable to have a solution to Problem 2, which is effective without requiring anything more than GAS and LES of the attractor for the attitude control system.
3) The solution should be implemented using (20a) that, through $\zeta(q, \omega)$, requires exact knowledge of the inertia J and may result in lack of robustness if J is uncertain.

These limitations can be overcome by following an alternative paradigm for the design of the stabilizing law, which arises from the intuition of reversing the cascaded structure of Fig. 2. This inversion of the cascade would result in the fact that the attitude stabilization would not be disturbed at all by the momentum dumping. In order to give priority to the attitude control goal, we revisit (13) and perform a different partition of the terms at the right-hand side in such a way that the disturbance d of the equivalent formulation (5) is zero

$$J\dot{\omega} + \omega^\times J\omega = \underbrace{-\tau_w - \omega^\times h_w + T_m}_{u}. \tag{22}$$

Then, the attitude dynamics (4b) and (22) corresponds to (4b) and (5) with $u = -\tau_w - \omega^\times h_w + T_m$ and $d = 0$. Following the same steps as in the previous section, the reaction wheels input τ_w can then be selected by only focusing on the attitude control goal using some global asymptotic stabilizer, such as the one discussed in Section II-B. In particular, with that construction, one can use (6) and select

$$\begin{aligned} \tau_w &= -\omega^\times h_w + T_m - u \\ &= -\omega^\times h_w - (R(q)\tilde{b}_\circ(t))^\times \tau_m - u \end{aligned} \tag{23}$$

[where we used (22) and (4c)]. Then, Lemma 1 implies that attitude stabilization is achieved globally, regardless of the torque T_m generated by the magentorquers.

As a next step, we can now focus on the momenta of the reaction wheels, which are indeed affected by the magnetorquers indirectly from the input selection (23). In particular,

[5] Note that in [25] forward completeness of all maximal solution is proven so all preasymptotic stability results are equivalent to asymptotic stability results.

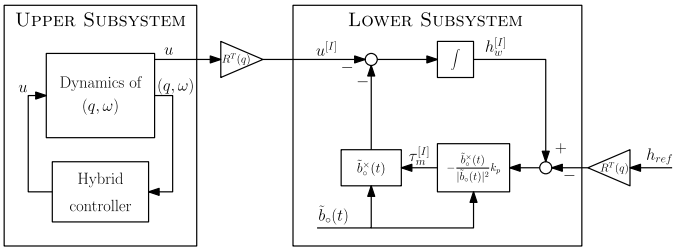

Fig. 4. Cascaded structure of the static allocation scheme.

using the second equation in (4a), selection (23), and the fact that h_{ref} is constant, we get

$$\dot{h_w - h_{\text{ref}}} = -\omega^\times h_w - u - (R(q)\tilde{b}_\circ(t))^\times \tau_m \tag{24a}$$

or

$$\dot{h}_w^{[I]} = -R^T(q)u - \tilde{b}_\circ^\times(t)\tau_m^{[I]} \tag{24b}$$

which reveals that the momentum of the reaction wheels is indeed affected by the attitude variables due to the presence of u at the right-hand side. Remarking that if $(q,\omega) \in \mathcal{A}$ then (24a) reduces to (15), it appears natural to select the magnetorquers input τ_m in such a way to exploit the useful stabilization result of Lemma 2, namely

$$\tau_m = -\frac{(R(q)\tilde{b}_\circ(t))^\times}{|\tilde{b}_\circ(t)|^2}k_p(h_w - h_{\text{ref}}) \tag{25a}$$

or

$$\tau_m^{[I]} = -\frac{\tilde{b}_\circ^\times(t)}{|\tilde{b}_\circ(t)|^2}k_p\big(h_w^{[I]} - R^T(q)h_{\text{ref}}\big) \tag{25b}$$

where k_p is a positive scalar gain.

The structure of the control loop is illustrated in Fig. 4 in order to make a thorough comparison with the structure represented in Fig. 2. The corresponding equations of the closed-loop system are composed of the control laws (6), (25b) and the upper subsystem

$$\begin{cases} (4b) \\ J\dot{\omega} + \omega^\times J\omega = u \end{cases} \tag{26}$$

which affects the lower subsystem (24b), (25b). This cascaded structure should be compared with (6), (20), and (21). In particular, comparing Fig. 4 with Fig. 2, it is obvious that we have exchanged the order of the attitude and momentum dumping subcomponents. As mentioned above, an advantage arising from the new cascaded structure of Fig. 4 is that the attitude control goal becomes the primary goal and is associated with transient responses that are not disturbed by the momentum dumping controller. Therefore, even though the limit set of the closed-loop trajectories is the same under both controllers, the solution of this section has no impact at all on the transient of the attitude dynamics. This feature is well illustrated by the simulation examples of Section V.

Theorem 2: Under Assumption 1, given any set of gains $k_p > 0$, $K_\omega = K_\omega^T \succ 0$, $c > 0$, and $\delta \in (0,1)$, consider the closed-loop system between plant (4) and controller (6), (23), (25a) with state space variables $x = (q, \omega, x_c, h_w)$. Then, the set $\mathcal{A}_e = \mathcal{A} \times \mathcal{A}_h$ as defined in (7) and (17) is GAS, namely the control scheme solves the formalization in Problem 2 of the engineering Problem 1.

Proof: The proof uses the results for asymptotic stability of nonlinear hybrid cascaded interconnections that have been recalled in the proof of Theorem 1 [namely [13, Corollary 19] and the follow-up results about the cascades [13, eq. (23)]]. In particular, generalizing to the hybrid case, the classical continuous-time result of [33], global asymptotic stability of the cascaded interconnection can be established using GAS and LES of the upper subsystem (which holds due to Lemma 1), 0-GAS of the lower subsystem (namely GAS with zero input), and global boundedness (GB) of trajectories. These three items are proven below.

1) *0-GES of the Lower Subsystem:* As already said, the zero input equation of the lower subsystem corresponds to (15) and (25a) [where it is recalled that $\tilde{b}(t) = R(q)\tilde{b}_\circ(t)$]. Thus, Lemma 2 can be directly applied to prove that $\mathcal{A}_h$ is globally exponentially stable for the lower subsystem with zero input.
2) *Global Boundedness:* By GB of the closed-loop (4), (6), (23), (25a), we mean that for each $r > 0$, there exists $\Psi(r) > 0$ such that[6] for each initial condition $x_0 = (\omega_0, q_0, x_{c0}, h_{w0})$ satisfying $|x_0|_{\mathcal{A}\times\mathcal{A}_h} \le r$, one has that all solutions x satisfy $|x(t,j)|_{\mathcal{A}\times\mathcal{A}_h} \le \Psi(r)$ for all $(t,j) \in \text{dom}(x)$. To show this, first note that GAS of the upper subsystem implies GB of the (ω, q, x_c) substate. As for the state h_w, consider the function $H = |\tilde{h}_w|^2/2$, where $\tilde{h}_w = h_w - h_{\text{ref}}$ and note that $\tilde{h}_w$ does not change across jumps, while along flows, from (24a), we get

$$\begin{aligned} \dot{H} &= \tilde{h}_w^T(-\omega^\times(\tilde{h}_w + h_{\text{ref}}) - \tilde{b}^\times(t)\tau_m - u) \\ &= -\tilde{h}_w^T(u + \omega^\times h_{\text{ref}}) + k_p\tilde{h}_w^T\frac{\tilde{b}^\times(t)\tilde{b}^\times(t)}{|\tilde{b}(t)|^2}\tilde{h}_w \end{aligned}$$

indeed $\tilde{h}_w^T\omega^\times\tilde{h}_w = -\tilde{h}_w^T\tilde{h}_w^\times\omega = 0$. Then, defining $\rho(t) := |u| + |\omega^\times h_{\text{ref}}|$ and remarking that $-\tilde{b}^\times(t)\tilde{b}^\times(t) = (\tilde{b}^\times(t))^T\tilde{b}^\times(t) \succeq \mathbf{0}, \forall t$, $\dot{H}$ can be bounded as follows:

$$\dot{H} \le |\tilde{h}_w|\ \rho(t) \le (1 + |\tilde{h}_w|^2)\rho(t) = (1 + 2H)\rho(t).$$

From GAS and LES of the (ω, q) dynamics, for each $r > 0$, there exist positive K_r, λ_r such that $\rho(t) \le K_r \exp(-\lambda_r t)$. Then, from Gronwall–Bellman's inequality [20, Lemma A.1], since $\rho(t)$ is integrable, we have that $H = |\tilde{h}_w|^2/2$ is globally bounded. ■

Let us now summarize the important advantages of using the new allocation-based scheme of this section as compared with the two approaches presented in Section III.

1) *Unmodified Transient of the Attitude Dynamics:* Bearing in mind that the scheme works for any attitude stabilizer inducing GAS and LES, the transient response induced by the preferred attitude stabilizer is preserved by the allocation-based scheme because the controlled attitude

[6] As customary, given a set $\mathcal{S}$ and vector w, we denote the distance of w from $\mathcal{S}$ as $|w|_{\mathcal{S}} := \inf_{z\in\mathcal{S}} |w - z|$.

dynamics is now the upper (undisturbed) block of the cascaded structure. Note that an interesting property induced by this feature is that the attitude stabilization is independent of $\tilde{b}(t)$ [or $\tilde{b}_\circ(t)$], which leads to more desirable robustness properties of the closed loop due to an intrinsic decoupling property.

2) *Only GAS and LES of the Attitude Stabilizer is Required:* As formally stated in the previous Theorem 2, global asymptotic stability of the attractor $\mathcal{A}_e$ holds under the mild requirement that the attitude stabilizer induce GAS and LES. This shows clear advantages as compared with: a) the classical approach, for which instability can be observed for an nonaggressive attitude stabilizer inducing GAS and LES and b) its revisited version, which requires an extra ISS property from the attitude stabilizer, as stated in Theorem 1. Note also that GAS of the attractor $\mathcal{A}_e$ implies uniform global convergence of the speed of the reaction wheels to the desired reference h_{ref}. Finally, it is also worthwhile mentioning that the stability properties guaranteed for the allocation-based scheme hold globally. In other terms, this means that the proposed strategy can be suitably employed when dealing with either large or small depointings. To the best of our knowledge, nothing can be said about the classical scheme with respect to this.

3) *Dealing With Saturations:* Regarding saturation of input torques and reaction wheels speed, the allocation-based scheme is preferable as compared with the classical one for two reasons. First, a formal proof of stability demonstrates that, with the allocation-based scheme, h_w converges to the arbitrary set point h_{ref}, which, when suitably defined, helps keeping h_w away from the saturation bounds and from zero velocity, which induces undesirable stiction effect. Second, global stability with the new scheme is guaranteed regardless of the aggressiveness of the attitude stabilizer. This allows implementing low-gain attitude controllers, less inclined to induce saturation of h_w, τ_w, and τ_m. Simulation results proposed in Section V confirm that this property does not hold for the classical scheme.

4) *Robustness With Respect to Model Parameters:* In the case where $\tilde{b}(t)$ is measured on board, the new control law is independent of the model parameters. This was not the case in the revisited version of the classical approach, where J is required.[7] This may be easily shown by comparing (25a) with (20a) where, in this last case, the dependence upon the inertia matrix J comes through the term $\zeta(q, \omega)$. This remark is an argument in favor of the robustness of the proposed allocation scheme as explained in [37].

V. Simulation Results

To suitably illustrate the control schemes proposed in this paper, we provide in this section a range of numerical simulations. All the simulation tests are carried out using the physical parameters of the satellite Demeter [27] designed and produced by CNES, the French space agency. This spacecraft is the first microsatellite in the Myriade series, a new concept of modular satellite weighing <200 kg, flying at an altitude of 710 km, and developed to provide an affordable access to space. Launched on June 29, 2004, the Demeter mission has now come to its end and the satellite was terminated on December 9, 2010. Like most low orbit satellites, Demeter is equipped with reaction wheels and magnetorquers. A star tracker is used to measured its attitude. All numerical data and specifications were provided by CNES [27] and correspond to the ones used for the real design of the control system implemented on board during the flight of Demeter. For simplicity of the exposition, the Demeter example is used here for an inertial pointing mission (as graphically shown in Fig. 1), whereas the real mission needed geocentric pointing. The inertia matrix is given by

$$J = \begin{bmatrix} 39.30 & -3.65 & -0.37 \\ -3.65 & 27.15 & -1.45 \\ -0.37 & -1.45 & 46.54 \end{bmatrix} \quad (\text{kg} \cdot \text{m}^2).$$

The nominal angular momentum of each reaction wheel is chosen to be 0.06 N $\cdot$ m $\cdot$ s, so that the constant vector h_{ref} is given by $0.06 \cdot [1, 1, 1]^T$. The actuators need to comply with the following constraints:

$$|h_w^i| \leq 2h_{\text{ref}}^i = 0.12 \text{ N} \cdot \text{m} \cdot \text{s}, \quad |\tau_w^i| \leq 0.005 \text{ N} \cdot \text{m}$$
$$|\tau_m^i| \leq 12 \text{ A} \cdot \text{m}^2 \quad \forall\, i = 1, 2, 3.$$

The circular orbit considered for the satellite is characterized by an altitude of 660 km, an inclination of 98.23°, and a local time of the ascending node of 22h15. From these parameters, the geomagnetic field $\tilde{b}_\circ(t)$ is evaluated using the IGRF model. Fig. 5 shows the chronograph of $\tilde{b}_\circ$ over a time range of 60 orbits, together with its periodic approximation. It is emphasized that in [35], we investigated the stability properties of our schemes under a periodicity assumption for $\tilde{b}_\circ$. Fig. 5 well illustrates the relevance of the extension, carried out in this paper, to nonperiodic instances of $\tilde{b}_\circ$. In Fig. 5, as well as in all the other figures reported in this section, we use the following color codes: the x-component is shown in blue, the y-component is shown in red, and the z-component is shown in green.

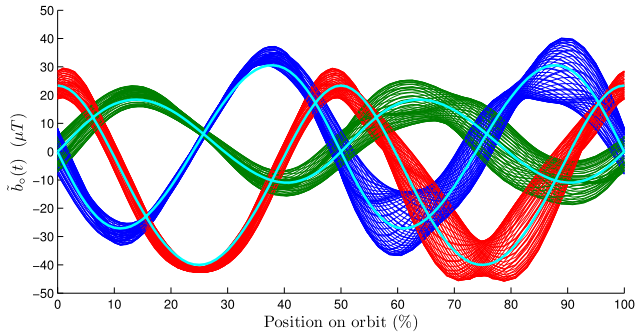

Fig. 5. Chronograph of $\tilde{b}_\circ$ together with its periodic approximation (thick cyan line) over 60 orbits.

[7] It should be, however, stated that the original classical cross-product control law does not require the knowledge of J.

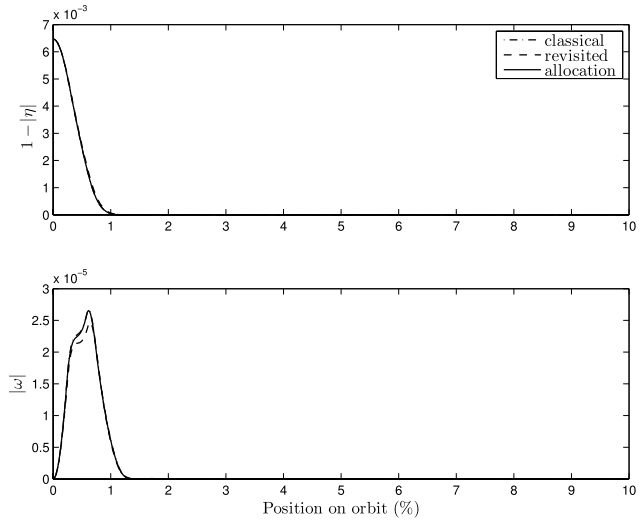

Fig. 6. Quaternion and ω for the three approaches using an aggressive attitude controller.

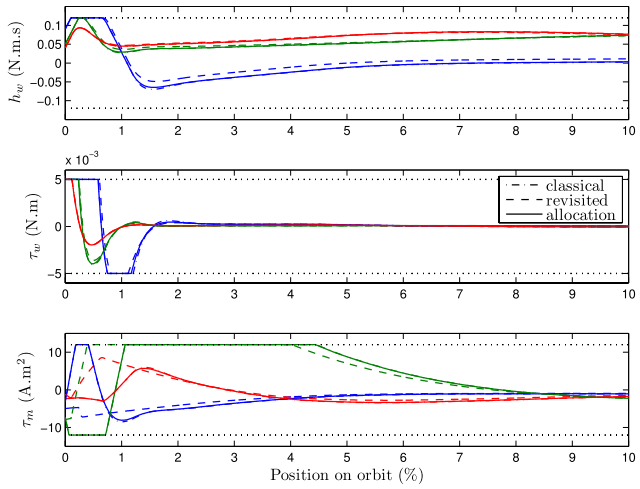

Fig. 7. h_w, τ_w, and τ_m for the three approaches using an aggressive attitude controller.

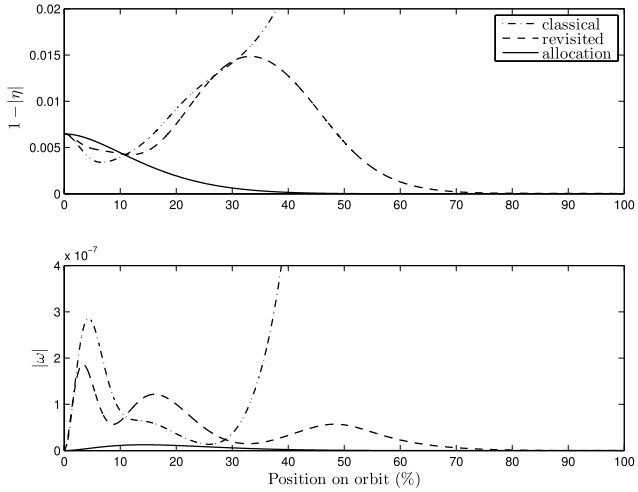

Fig. 8. Quaternion and ω for the three approaches using a nonaggressive attitude controller.

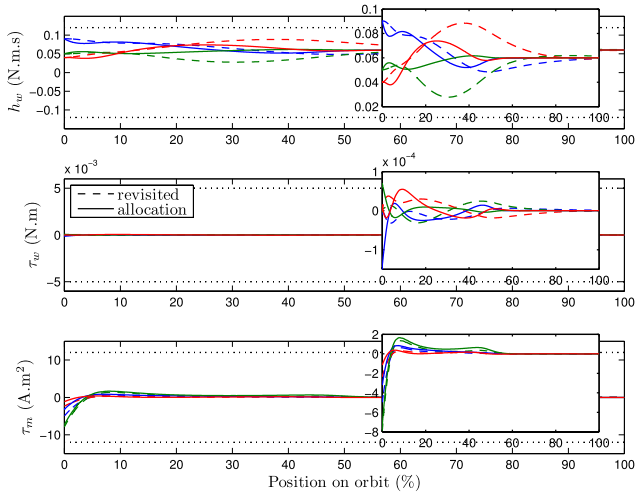

Fig. 9. h_w, τ_w, and τ_m (with zoomed-in-view) using a nonaggressive attitude controller for the revisited and the allocation-based strategies.

Several stabilization problems with non-nominal initial angular momentum of the wheels have been simulated using the control laws presented in this paper, namely:

1) the classical approach (dash-dotted lines in our figures);
2) its revisited version (dashed lines);
3) the allocation-based strategy (solid lines).

For all our simulations, unless differently specified, the initial conditions are selected as $h_{w0} = [0.09, 0.05, 0.04]^T$, $\omega_0 = \mathbf{0}$, $\epsilon_0 = [0.10, 0.05, 0.02]^T$, and $\eta_0 = (1 - \epsilon_0^T \epsilon_0)^{1/2}$.

Regarding the parameter k_p-inducing momentum dumping, keeping in mind that it should be strictly positive, we ran several numerical simulations of the closed loop (15) with (16). The resulting choice was $k_p = 5 \cdot 10^{-3}$. Remarkably, choosing larger or smaller values leads to deteriorated responses, which reveals somewhat interesting trends of the linear time-varying stabilizing law (16).

1) Aggressive Attitude Stabilizer: As a first test, the parameters of the hybrid attitude stabilizer u defined by (6) are chosen to make this control law aggressive: we assign $K_\omega = 5 \cdot \mathbf{1}_3$ and $c = 0.5$. Additionally, $x_{c_0} = 1$ and $\delta = 0.5$. The simulation results are displayed in Figs. 6 and 7. While all closed-loop systems eventually converge to the desired attitude equilibrium for all control strategies, it can be seen that all the actuators signals, namely h_w, τ_w, and τ_m, hit the saturation limits (dotted horizontal lines). This is the main drawback of selecting an aggressive attitude stabilizer. Note that using an aggressive attitude controller induces comparable responses on all of the three proposed schemes. We will point out that this is not the case when studying the responses in the presence of disturbances, as illustrated at the end of the section.

2) Nonaggressive Attitude Stabilizer: In a subsequent simulation test, to prevent saturation, the attitude stabilizer parameters are redefined in order to obtain an attitude controller that is less demanding for the actuators. In particular, we choose the smaller values $c = 10^{-4}$ and $K_\omega = 0.07 \cdot \mathbf{1}_3$, whereas δ and x_{c_0} remain unchanged. The simulation results starting from the same initial conditions are displayed in Figs. 8 and 9. From Fig. 8, it appears that the classical (dash-dotted line) controller leads to instability as one would expect in light of the discussions already provided in Remark 4. Instead, the other control strategies ensure convergence to the equilibrium

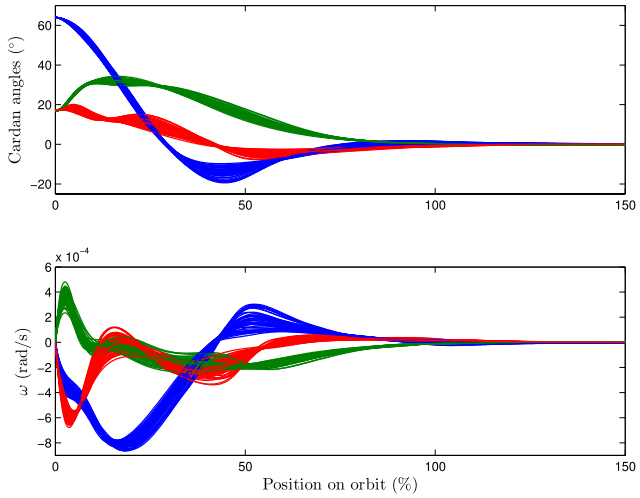

Fig. 10. Monte Carlo study on uncertainties on J. Cardan angles and w for the revisited controller.

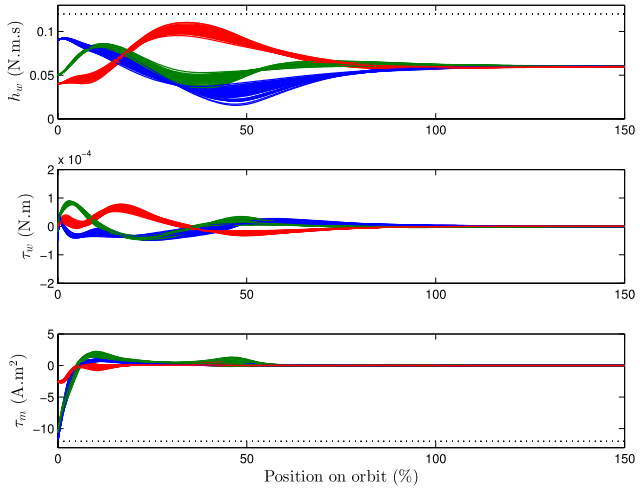

Fig. 11. Monte Carlo study on uncertainties on J. h_w, τ_w, and τ_m for the revisited controller.

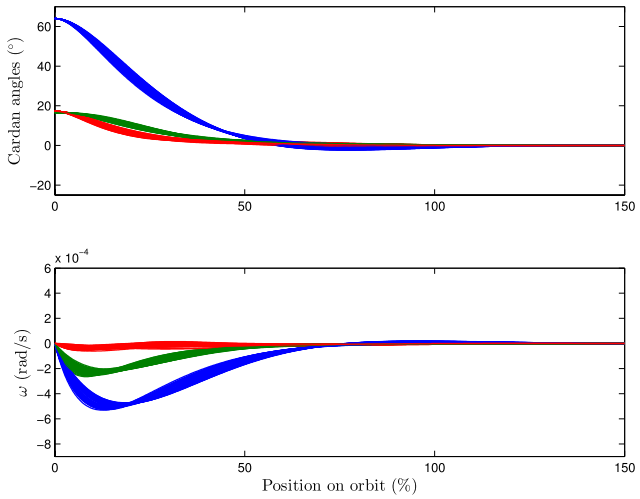

Fig. 12. Monte Carlo study on uncertainties on J. Cardan angles and w for the allocation-based controller.

(as predicted by Theorems 2 and 1) without reaching the actuators limits. Finally, one can observe that the time evolution of (ω, q) is more regular with the allocation scheme than it is with the revisited approach. This result is expected as it originates from the hierarchical relationship between the two stabilization tasks, represented in Fig. 4, where the attitude control loop is independent of the momentum dumping task so that the allocation control law intrinsically prevents the transient of the reaction wheels desaturation loop from introducing disturbances on the attitude transient.

3) Influence of the Uncertainties on the Model Parameters: Based on the observations already mentioned in Remark 1, the asymptotic stability properties established in this paper are robust to disturbances of the plant dynamics. In light of this fact, using the same nonaggressive attitude stabilizer, a set of Monte Carlo simulations has been performed to evaluate the sensitivity of each control scheme to variations of J. In particular, following the benchmark definition proposed in [27], the Monte Carlo extractions for the randomized analysis have been carried out using a uniform distribution of the parameters of J within the following disturbance ranges: ± 3 kg $\cdot$ m^2 on the off-diagonal terms and $\pm 30\%$ on the three diagonal terms. The random disturbed inertia matrix J has been used in place of the nominal one in the satellite dynamics (4) (while the inertia matrix used by the controllers, wherever needed, remains the nominal one). Figs. 10–13 show the simulation results using 50 such Monte Carlo extractions for the revisited and the allocation controllers (the response with the classical controller diverges also in this case). Note that larger initial depointings are now considered, namely $\epsilon_0 = [0.50, 0.20, 0.05]^T$ and $\eta_0 = (1 - \epsilon_0^T \epsilon_0)^{1/2}$, whereas $h_{w0} = [0.09, 0.05, 0.04]^T$ and $\omega_0 = \mathbf{0}$ remain the same.

The fact that both of the proposed closed-loop systems behave well and do not reach the saturation limits for all of the considered disturbances of J, is a practical illustration of the robustness of these approaches. On the other hand, from a theoretical viewpoint, some level of robustness can be guaranteed from the regularity of the hybrid system data using the results in [14, Ch. 6 and 7] (see also Remark 1). In the case of the allocation-based controller, these observations were predicted by Theorem 2 as this control scheme is independent of J, which means that closed-loop GAS holds for any positive definite selection of J. This is in contrast to the revisited strategy for which the same kind of robustness result seems to be much harder to establish, and might even not hold in general. As for the previous case, one can again observe, by comparing Figs. 10 and 12, that the allocation-based solution leads to more regular responses due to the advantages arising from the underlying cascaded scheme that prioritizes the attitude stabilization task.

4) Rejection of Periodic Disturbances: To assess the performance of the proposed controller in a more realistic environment, a disturbing torque T_{ext} is injected in the dynamics and comparisons between the classical and the allocation schemes are given via a new set of simulations. Predominant for LEO, as in the Demeter example [27], gravity gradient disturbances, aerodynamic drag, and magnetic torques disturbances caused by the interaction of the current loops with the magnetic field, can be modeled in the inertial frame by two periodic signals T_1 and T_2, whose period is one and two times the orbital

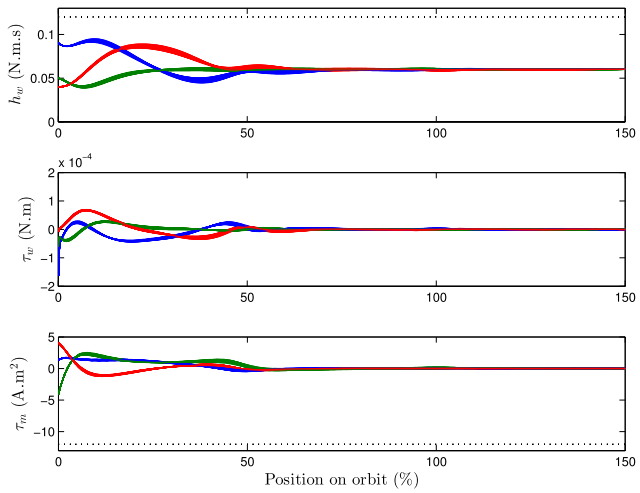

Fig. 13. Monte Carlo study on uncertainties on J. h_w, τ_w, and τ_m for the allocation-based controller.

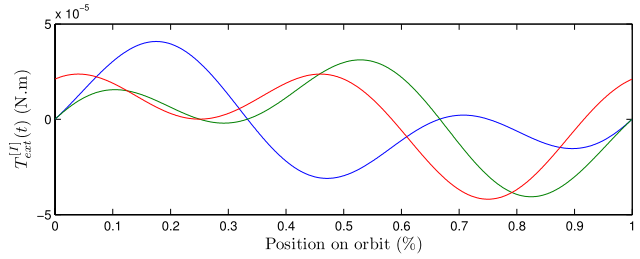

Fig. 14. Periodic disturbance $T_{\text{ext}}^{[I]}$ used for the simulations of Figs. 15 and 16.

frequency ω_0 added to a secular term T_0 [7], [34]

$$T_{\text{ext}}^{[I]}(t) = \begin{bmatrix} T_{0x} + T_{1x}\sin(\omega_0 t + \varphi_{1x}) + T_{2x}\sin(2\omega_0 t + \varphi_{2x}) \\ T_{0y} + T_{1y}\sin(\omega_0 t + \varphi_{1y}) + T_{2y}\sin(2\omega_0 t + \varphi_{2y}) \\ T_{0z} + T_{1z}\sin(\omega_0 t + \varphi_{1z}) + T_{2z}\sin(2\omega_0 t + \varphi_{2z}) \end{bmatrix}. \quad (27)$$

The dynamic equation (4a) is then modified accordingly and corresponds to

$$J\dot{\omega} + \omega^{\times}(J\omega + h_w) = -\tau_w + T_m + R(q)T_{\text{ext}}^{[I]}(t). \quad (28)$$

Simulations have been performed over 20 orbits using the aggressive attitude stabilizer previously introduced and are reported in Figs. 15 and 16. For these simulations, according to [7] and [34], the numerical parameteres in (27) have been selected as follows: $T_{0x} = T_{0y} = T_{0z} = 1 \cdot 10^{-7}$ (N $\cdot$ m), $T_{1x} = T_{1y} = T_{1z} = 2.1 \cdot 10^{-5}$ (N $\cdot$ m), $T_{2x} = T_{2y} = T_{2z} = 2.1 \cdot 10^{-5}$ (N $\cdot$ m), $\varphi_{T1x} = -\varphi_{T2x} = \pi/4$, $\varphi_{T1y} = -\varphi_{T2y} = -\pi/4$, $\varphi_{T1z} = 0$, and $\varphi_{T2z} = \pi/2$. This corresponds to the periodic trace for the overall disturbance $T_{\text{ext}}^{[I]}$ represented in Fig. 14.

To remain coincise, only the attitude responses variables are displayed in Figs. 15 and 16. Indeed, the two control schemes lead to very similar behavior of the actuators signals (namely h_w, τ_w, and τ_m) that exhibit an oscillatory behavior that remains well within the saturation limits. The most relevant insight coming from this last set of simulation is revealed by a comparative evaluation of the attitude variables

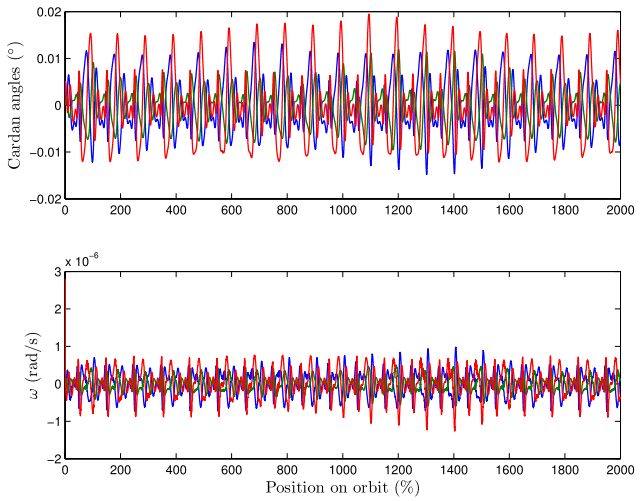

Fig. 15. Attitude reponses (Cardan angles and w) to a periodic disturbance using the classical controller.

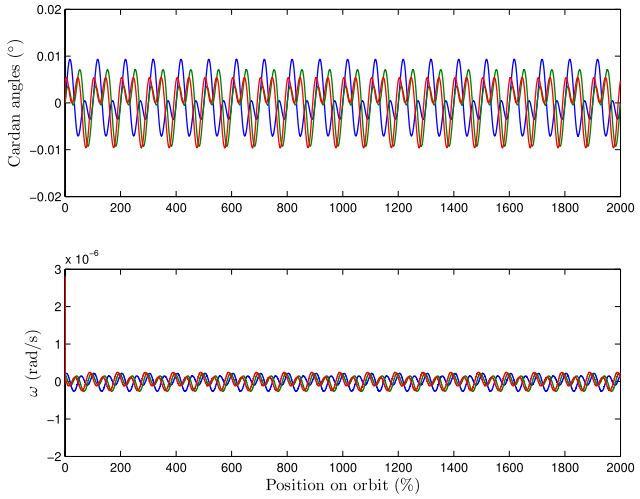

Fig. 16. Attitude reponses (Cardan angles and w) to a periodic disturbance using the allocation-based controller.

of Figs. 15 and 16. Indeed, the advantages arising from the cascaded structure of the allocation-based solution (see Fig. 4), where the allocation closed loop is completely independent of $\tilde{b}_\circ$, can be well appreciated in Fig. 16, where the attitude is only affected by the periodic external disturbance torque $T_{\text{ext}}^{[I]}$ and the attitude variables converge to a periodic steady state. Conversely, for the structure in Fig. 2 of the classical strategy, the attitude variables are affected by both $T_{\text{ext}}^{[I]}$ and the nonperiodic term $\tilde{b}_\circ$ (Fig. 5). As a result, the behavior of the attitude variables is nonperiodic.

Finally, it should be noted that from the two block diagrams of Figs. 2 and 4, the attitude of the classical controller is disturbed by its feedback interaction with the momentum dumping dynamics. This fact explains the larger irregular oscillations that can be appreciated by comparing Figs. 15 and 16.

VI. Conclusion

In this paper, the problem of designing an attitude stabilizer for satellites equipped with a set of magnetorquers and reaction

wheels is dealt with. The classical cross-product control law addressing this problem is first investigated and its hidden assumptions are revealed. Then, this control scheme is revisited to obtain a new control strategy benefiting from a rigorous proof of global asymptotic stability and local exponential stability under reasonable assumptions on the geomagnetic field. Relying on this preliminary study, a new allocation-based control scheme is finally proposed as the main contribution of this paper. In addition to the features of the revisited controller, the allocation-based strategy makes the attitude dynamics independent of the momentum dumping task. This is highly desirable as it allows to completely decouple the design of the attitude stabilizer from its implementation problem in satellites with the considered dual actuator configuration.

APPENDIX

PROOF OF LEMMA 2

Using $b_\circ(t) = \tilde{b}_\circ(t)/|\tilde{b}_\circ(t)|$ as defined before Assumption 1, we can rewrite the closed loop (15) and (16) with $\tilde{b}$ replaced by $\tilde{b}_\circ$ as follows:

$$\dot{\tilde{h}}_w = k_p b_\circ^\times(t) b_\circ^\times(t) \tilde{h}_w \tag{29}$$

where we use for simplicity $\tilde{h}_w = h_w - h_{\text{ref}}$. Then, in the transformed coordinates, the lemma is proved if we establish UGES of the origin for (29).

We first introduce the candidate Lyapunov function proposed by [23, Proposition 1]

$$V(t, \tilde{h}_w) = \tilde{h}_w^T \left(\frac{\lambda}{2} \mathbf{1}_3 - M(t) \right) \tilde{h}_w \tag{30}$$

where $M(t)$ has been defined in (9)–(11). From the boundedness of $M(t)$, coming from Assumption 1, and for a large enough $\lambda > 0$, V satisfies, for all $\tilde{h}_w$ and for some positive scalars c_1, c_2

$$c_1 |\tilde{h}_w|^2 \leq V(t, \tilde{h}_w) \leq c_2 |\tilde{h}_w|^2 \quad \forall t \geq 0. \tag{31}$$

We can then compute its derivative along dynamics (29) as

$$\dot{V}(t, \tilde{h}_w) = -(\tilde{h}_w)^T Q(t) \tilde{h}_w \tag{32}$$

with

$$Q(t) = (-\lambda \mathbf{1}_3 + 2M(t)) k_p b_\circ^\times(t) b_\circ^\times(t) + b_\circ(t) b_\circ^T(t) - \Pi_\infty.$$

The two unit vectors $b_1(t)$, $b_2(t)$ are now introduced. They form an orthogonal basis with $b_\circ(t)$, i.e., defining $T(t) = [\, b_0(t) \; b_1(t) \; b_2(t) \,]$, we have $T^T(t)T(t) = \mathbf{1}_3$. Then, from the definition of $M(t)$, it is readily seen that $\tilde{Q}(t) := T^T(t) Q(t) T(t)$ corresponds to

$$\tilde{Q}(t) = \begin{bmatrix} 1 & 0 & 0 \\ 0 & \lambda k_p & 0 \\ 0 & 0 & \lambda k_p \end{bmatrix} - k_p \left(\left[\begin{array}{c|cc} 0 & & \\ 0 & & \Xi(t) \\ 0 & & \end{array}\right] + \left[\begin{array}{ccc} 0 & 0 & 0 \\ \hline & \Xi^T(t) & \end{array}\right] \right) - T^T(t) \Pi_\infty T(t)$$

with $|\Xi(t)| = |T^T(t) M(t) [b_1(t) \;\; b_2(t)]| \leq \sigma$. Now, from the rightmost inequality of (10), in Assumption 1, there exists a positive scalar γ such that $\Pi_\infty \preceq (1 - \gamma) \mathbf{1}_3$. Therefore, $T^T(t) \Pi_\infty T(t) \preceq (1 - \gamma) T^T(t) T(t) = (1 - \gamma) \mathbf{1}_3$ and there exists a large enough $\lambda > 0$ such that $\tilde{Q}(t) \geq c_3 \mathbf{1}_3$ for some positive scalar c_3, which implies $Q(t) \geq c_3 \mathbf{1}_3$. Finally, from (32), we get $\dot{V}(t, \tilde{h}_w) \leq -c_3 |\tilde{h}_w|^2$ which, together with (31) implies UGES of the origin for (29) by [20, Th. 4.10].

ACKNOWLEDGMENT

The authors would like to thank A. Astolfi and M. Lovera for their insightful comments regarding the observations in Remark 2.

REFERENCES

[1] S. P. Bhat and D. S. Bernstein, "A topological obstruction to continuous global stabilization of rotational motion and the unwinding phenomenon," *Syst. Control Lett.*, vol. 39, no. 1, pp. 63–70, Jan. 2000.

[2] C. Cai and A. R. Teel, "Characterizations of input-to-state stability for hybrid systems," *Syst. Control Lett.*, vol. 58, no. 1, pp. 47–53, Jan. 2009.

[3] P. J. Camillo and F. L. Markley, "Orbit-averaged behavior of magnetic control laws for momentum unloading," *J. Guid. Control*, vol. 3, no. 6, pp. 563–568, Nov./Dec. 1980.

[4] C. K. Carrington, W. A. Baracat, and J. L. Junkins, "A comparative study of magnetic mometum dump laws," in *Proc. AAS/AIAA Astrodyn. Conf.*, Lake Tahoe, NV, USA, Aug. 1981.

[5] N. A. Chaturvedi, A. K. Sanyal, and N. H. McClamroch, "Rigid-body attitude control," *IEEE Control Syst.*, vol. 31, no. 3, pp. 30–51, Jun. 2011.

[6] X. Chen, W. H. Steyn, S. Hodgart, and Y. Hashida, "Optimal combined reaction-wheel momentum management for earth-pointing satellites," *J. Guid., Control, Dyn.*, vol. 22, no. 4, pp. 543–550, Aug. 1999.

[7] M. Courtois, *Space Technology Course—Spacecraft Techniques and Technology—Volume 3: Platforms, Module XII: Attitude Control and Pointing*. Toulouse, France: Cepadues-editions, 2005.

[8] J. H. Decanini, H. Flashner, and H. Schmeichel, "Magnetic control and the 25 kW power system," in *Proc. Annu. Rocky Mountain Guid. Control Conf.*, vol. 45. 1981.

[9] D. Desiderio, M. Lovera, S. Pautonnier, and R. Drai, "Magnetic momentum management for a geostationary satellite platform," *IET Control Theory Appl.*, vol. 3, no. 10, pp. 1370–1382, Oct. 2009.

[10] J. R. Forbes and C. J. Damaren, "Geometric approach to spacecraft attitude control using magnetic and mechanical actuation," *J. Guid., Control, Dyn.*, vol. 33, no. 2, pp. 590–595, Mar./Apr. 2010.

[11] S. Galeani, A. Serrani, G. Varano, and L. Zaccarian, "On linear over-actuated regulation using input allocation," in *Proc. 50th IEEE CDC-ECC*, Orlando, FL, USA, Dec. 2011, pp. 4771–4776.

[12] F. Giulietti, A. Quarta, and P. Tortora, "Optimal control laws for momentum-wheel desaturation using magnetorquers," *J. Guid., Control, Dyn.*, vol. 29, no. 6, pp. 1464–1468, Nov./Dec. 2006.

[13] R. Goebel, R. G. Sanfelice, and A. R. Teel, "Hybrid dynamical systems," *IEEE Control Syst.*, vol. 29, no. 2, pp. 28–93, Apr. 2009.

[14] R. Goebel, R. G. Sanfelice, and A. R. Teel, *Hybrid Dynamical Systems: Modeling, Stability, and Robustness*. Princeton, NJ, USA: Princeton Univ. Press, 2012.

[15] H. B. Hablani, "Pole-placement technique for magnetic momentum removal of earth-pointing spacecraft," *J. Guid., Control, Dyn.*, vol. 20, no. 2, pp. 268–275, Mar. 1997.

[16] P. C. Hugues, *Spacecraft Attitude Dynamics*. New York, NY, USA: Dover, 1986.

[17] Z. P. Jiang, A. R. Teel, and L. Praly, "Small-gain theorem for ISS systems and applications," *Math. Control, Signals, Syst.*, vol. 7, no. 2, pp. 95–120, 1994.

[18] T. A. Johansen and T. I. Fossen, "Control allocation—A survey," *Automatica*, vol. 49, no. 5, pp. 1087–1103, 2013.

[19] S. M. Joshi, A. G. Kelkar, and J. T. Y. Wen, "Robust attitude stabilization of spacecraft using nonlinear quaternion feedback," *IEEE Trans. Autom. Control*, vol. 40, no. 10, pp. 1800–1803, Oct. 1995.

[20] H. Khalil, *Nonlinear Systems*, 3rd ed. Upper Saddle River, NJ, USA: Prentice-Hall, 2002.

[21] A. Loria and E. Panteley, "Stability, told by its developers," in *Advanced Topics in Control Systems Theory* (Lecture Notes in Control and Information Science), vol. 328, A. Loria, F. Lamnabhi-Lagarrigue, and E. Panteley, Eds. London, U.K.: Springer-Verlag, 2006, pp. 199–258.

[22] M. Lovera, "Optimal magnetic momentum control for inertially pointing spacecraft," *Eur. J. Control*, vol. 7, no. 1, pp. 30–39, 2001.
[23] M. Lovera and A. Astolfi, "Spacecraft attitude control using magnetic actuators," *Automatica*, vol. 40, no. 8, pp. 1405–1414, Aug. 2004.
[24] M. Lovera and A. Astolfi, "Global magnetic attitude control of inertially pointing spacecraft," *J. Guid., Control, Dyn.*, vol. 28, no. 5, pp. 1065–1072, 2005.
[25] C. G. Mayhew, R. G. Sanfelice, and A. R. Teel, "Robust global asymptotic attitude stabilization of a rigid body by quaternion-based hybrid feedback," in *Proc. 28th IEEE Conf. CDC/CCC*, Shanghai, China, Dec. 2009, pp. 2522–2527.
[26] R. J. McElvain, "Satellite angular momentum removal utilizing the earth's magnetic field," in *Torques and Attitude Sensing in Earth Satellites*, S. F. Singer, Ed. New York, NY, USA: Academic, 1964, pp. 137–158.
[27] C. Pittet and D. Arzelier, "Demeter: A benchmark for robust analysis and control of the attitude of flexible icrosatellites," in *Proc. IFAC Symp. Robust Control Des.*, Toulouse, France, 2006.
[28] C. Pittet and C. Fallet, "Gyroless attitude control of a flexible microsatellite," in *Proc. 5th Conf. Dyn. Control Syst. Struct. Space*, Cambridge, U.K., 2001.
[29] R. Schlanbusch, A. Loria, and P. J. Nicklasson, "On the stability and stabilization of quaternion equilibria of rigid bodies," *Automatica*, vol. 48, no. 12, pp. 3135–3141, Dec. 2012.
[30] A. Serrani, "Output regulation for over-actuated linear systems via inverse model allocation," in *Proc. IEEE 51st Annu. CDC*, Maui, HI, USA, Dec. 2012, pp. 4871–4876.
[31] A. Serrani and M. Bolender, "Invited session: Control of over-actuated systems: Application to guidance and control of aerospace, marine and terrestrial vehicles," in *Proc. 14th Medit. Conf. Control Autom.*, Ancona, Italy, Jun. 2006.
[32] M. J. Sidi, *Spacecraft Dynamics and Control: A Practical Engineering Approach*. Cambridge, U.K.: Cambridge Univ. Press, 1997.
[33] E. D. Sontag, "Remarks on stabilization and input-to-state stability," in *Proc. 28th IEEE Conf. Decision Control*, Tampa, FL, USA, Dec. 1989, pp. 1376–1378.
[34] J.-F. Trégouët, D. Arzelier, D. Peaucelle, Y. Ebihara, C. Pittet, and A. Falcoz, "Periodic H_2 synthesis for spacecraft attitude control with magnetorquers and reaction wheels," in *Proc. 50th IEEE CDC-ECC*, Orlando, FL, USA, Dec. 2011, pp. 6876–6881.
[35] J. F. Trégouët, D. Arzelier, D. Peaucelle, and L. Zaccarian, "Static input allocation for reaction wheels desaturation using magnetorquers," in *Proc. 19th IFAC Symp. Autom. Control Aerosp.*, Wuerzburg, Germany, Sep. 2013.
[36] J. F. Trégouët, D. Arzelier, D. Peaucelle, and L. Zaccarian, "Reaction wheels desaturation using magnetorquers and static input allocation," LAAS-CNRS, Paul Sabatier Univ., Toulouse, France, Tech. Rep. 13472, Nov. 2013.
[37] J. T. Y. Wen and K. Kreutz-Delgado, "The attitude control problem," *IEEE Trans. Autom. Control*, vol. 36, no. 10, pp. 1148–1162, Oct. 1991.
[38] J. R. Wertz, *Spacecraft Attitude Determination and Control*. Norwell, MA, USA: Kluwer, 1978.
[39] L. Zaccarian, "Dynamic allocation for input-redundant control systems," *Automatica*, vol. 45, no. 6, pp. 1431–1438, Jun. 2009.
[40] K. Zhou, J. C. Doyle, and K. Glover, *Robust and Optimal Control*. Englewood Cliffs, NJ, USA: Prentice-Hall, 1998.

Jean-François Trégouët received the M.S. degree in electrical engineering from the University of Sherbrooke, Sherbrooke, QC, Canada, the Dipl.Ing. degree from Ecole Supérieure d'Electronique de l'Ouest, Angers, France, in 2009, and the Ph.D. degree from the Laboratoire d'Analyse et d'Architecture des Systèmes, Centre National de la Recherche Scientifique, Toulouse, France, in 2012.

He was a Post-Doctoral Fellow with Curtin University, Bentley, WA, USA, in 2013. He is currently an Assistant Professor with the Institut National des Sciences Appliquées, Lyon, France, and a member of the Ampère Laboratory, Lyon. His current research interests include periodic systems, convex optimization over linear matrix inequalities, and attitude control of satellites.

Denis Arzelier was born in Villeneuve Saint Georges, France, in 1964. He received the Dipl.Ing. degree from Ecole Nationale Suprieure des Arts et Mtiers, Paris, France, in 1989, the D.E.A. (master's) degree in control from Ecole Centrale, Lille, France, in 1990, and the Ph.D. degrees from the Laboratoire dAnalyse et dArchitecture des Systemes, Centre National de la Recherche Scientifique (LAAS-CNRS), Toulouse, France, and the Institut National des Sciences Appliquées, Toulouse, in 1992.

He has been a Researcher at LAAS-CNRS since 1993. His current research interests include robust control, convex optimization, and optimal control for aerospace.

Dimitri Peaucelle was born in Leningrad, Russia, in 1974. He received the Ph.D. degree from the University of Toulouse, Toulouse, France, in 2000.

He is a full-time Researcher with the French National Center for Scientific Research, Paris, France, and is with the Laboratory for Analysis and Architecture of Systems, Toulouse. He is also involved in computer-aided control design activities and leads a project for control-oriented software development. He is the main contributor to the Robust Multiobjective Control Toolbox. He has been involved in several industrial projects with aerospace partners for launcher, aircraft, and satellite robust control. His current research interests include robust control, and extend to convex optimization over linear matrix inequalities, periodic systems, time-delay systems, and direct adaptive control.

Christelle Pittet received the Engineering degree in aeronautics from Ecole Nationale de l'Aviation Civile, Toulouse, France, in 1995, and the Ph.D. degree from the University Paul Sabatier of Toulouse, Toulouse, in 1998.

She has been with the French Space Agency, Toulouse, since 2000, as an Attitude and Orbit Control System expert, where she is in charge of advanced control studies, project development, and in-flight analysis.

Luca Zaccarian (M'09–SM'09) received the Laurea and Ph.D. degrees from the University of Roma "Tor Vergata," Rome, Italy, in 1995 and 2000, respectively.

He was an Assistant Professor in Control Engineering with the University of Roma "Tor Vergata" from 2000 to 2006 and became an Associate Professor. Since 2011, he has been the Directeur de Recherche with the Laboratoire d'Analyse et d'Architecture des Systèmes, Centre National de la Recherche Scientifique, Toulouse, France. Since 2013, he has also held a part-time position with the University of Trento, Trento, Italy. His current research interests include the analysis and design of nonlinear and hybrid control systems and their applications.

Prof. Zaccarian was a recipient of the 2001 O. Hugo Schuck Best Paper Award from the American Automatic Control Council.